J.G.Heinrich and C. Aneziris, Proc. 10th ECerS Conf., Göller Verlag, Baden-Baden, 2007, 942-947, ISBN: 3-87264-022-4

Kinetics of Hydroxyapatite Formation from Cuttlefish Bones

H. Ivankovic[1*], S. Orlic[1], E. Tkalcec[1], G.Gallego Ferrer[2]

[1]University of Zagreb, Faculty of Chemical Engineering and Technology, Croatia,
[2]Universitat Politecnica de Valencia, Centro de Biomaterialies, Valencia, Spain

Abstract

Hydrothermal method of synthesis hydroxyapatite scaffolds from aragonitic cuttlefish bones, (*Seppia Officinalis L.,* Adriatic Sea), at temperatures 180°C and 200°C for 1 to 48 hours is described. The phase composition of the bone and converted samples were examined by: X-ray diffraction and Fourier transform infrared spectroscopy. The rate of transformation was studied by quantitative X-ray diffraction using Rietveld refinement method, and Johnson-Mehl-Avrami approach was used to follow the transformation kinetics. The mechanism of hydroxyapatite formation could be defined as diffusion controlled growth of HAp crystals with the dominant growth along to the *c*-axis. FTIR spectroscopy determined B-type substitution of CO_3^{2-} groups, (i.e., on the tetrahedral PO_4^{3-} sites) into the structure. The microstructure of native and transformed bones was studied by scanning electron microscopy. The natural, porous and interconnected structure of bones maintained through the hydrothermal treatment, and hydroxyapatite crystals have needle like shape.

Introduction

Hydroxyapatite (HAp) with chemical formula $Ca_{10}(PO_4)_6(OH)_2$ is being extensively used for bioimplantion [1, 2]. Due to similarity in the mineral constituents with natural hard tissues (bones and teeth) it has excellent biocompatibility [2]. However, due to its low mechanical strength its usage is limited on phase reinforcement in composites, coatings on metal implants, granular fill for direct incorporation into human tissues and recently on production of porous scaffolds which can host the biological activities in a physiological manner [3]. Non-medical applications of porous Hap ceramics include packing media for column chromatography, gas sensors, catalyst and host materials [4] Rapid prototyping [5] or the foaming agents [6] have been employed to produce porous scaffolds of synthetic hydroxyapatite. However, the methods are expensive and not well defined with respect to internal porous architecture. Several attempts to convert natural aragonite structures (e.g., corals, nacres, etc.) hydrothermally to hydroxyapatite have been reported [7,8]. The ability of fast transformation of natural aragonitic ($CaCO_3$) structure into Hap, even at room temperature, has been shown by Ni et al [9]. Rocha et al. [3, 10, 11] were the first who performed the hydrothermal transformation of aragonitic cuttlefish bones into HAp. The inorganic part of cuttlefish bone (also called cuttlebone) is a lamellar mineralized porous structure of aragonite. Its highly channeled structure favors the diffusion of the reaction solution towards the aragonite and its fast transformation into HAp. Various mechanisms of transformation of $CaCO_3$ into HAp are assumed in literature. W. Eysel and D. Roy [12] proposed topotactic reaction of aragonite to HAp, dissolution and precipitation reaction of aragonitic nacres to HAp was proposed by Ni et al [9]. Zaremba et al [13], studying the aragonite transformation in gastropod (abalone) nacres, suggested dissolution-recrystallization mechanism of the HAp growth, whereas Yoshimura et al. [14], proposed dissolution-precipitation mechanism followed by nucleation and growth of HAp on the surface of $CaCO_3$.

The aim of the work was: to follow the kinetics of aragonitic cuttlefish bones transformation into HAp in dependence of temperature and time of hydrothermal treatment using Johnson- Mehl-Avrami [15,16] model, which describes the nucleation and growth of crystals from amorphous materials.

Materials and methods

The cuttlefish bones (*Seppia Officinalis L,* from Adriatic Sea) heated at 350°C for 3 h, (to remove organic materials)were used as the starting materials. For hydrothermal treatment only the peaces cut out from internal cuttlebone matrix (lamellae spacing) were used, since by the pre-treatment at 350°C the aragonite in external wall (dorsall shield) transforms into calcite. The content of aragonite ($CaCO_3$) in cuttlebones was determined by DTA-TG analysis. Small peaces of bones (about 2 cm^3) were poured with the required volume of an aqueous solution of 0.6M $NH_4H_2PO_4$ (Ca/P =1.67) in teflon lined stainless steel pressure vessel and sealed at 180 and 200°C for various times (1 to 48 hours) in the electric furnace. The converted peaces were washed with boiling water and dried at 110°C. The micro-structure of heated (350°C) and hydrothermal treated (HT) cuttlefish bones have been examined by scanning electron microscopy (SEM ISIDS-130).The conversion of HT transformation was followed by X-ray diffraction analysis (Philips PW 1820 counter diffractometer with Cu Kα radiation). Changes of crystal structure and unit cell parameters of HAP upon heating were followed by Rietveld structure refinement approach [17] carried out on XRD patterns collected from 15 to 120° 2θ, with steps of 0.02° and with fixed counting time of 10 seconds per step.

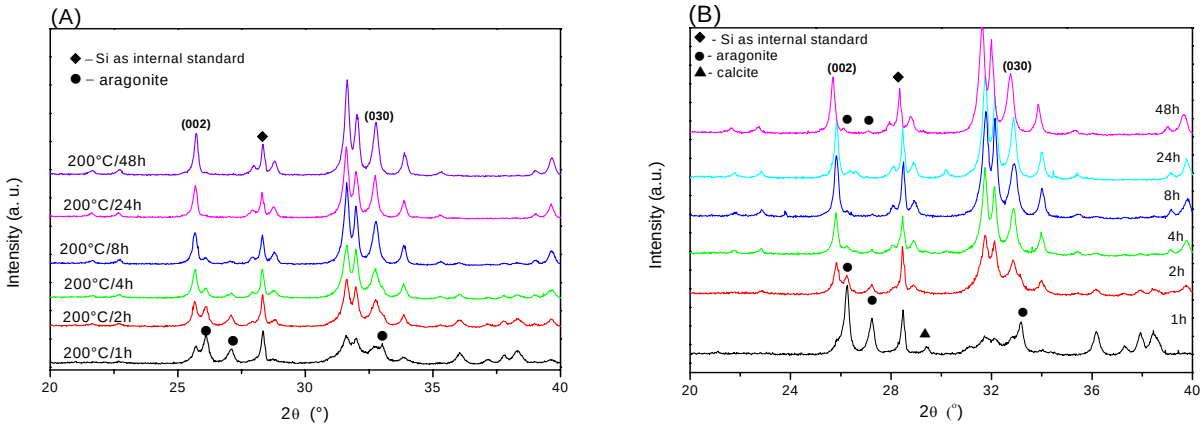

Fig. 1. XRD patterns of hydrothermal treated peaces of cuttlefish bone: (A) at 200°C and (B) at 180°C. ◆–added as internal standard; ●–aragonite; ▲– calcite

The software Topas 2.1 [18] (Bruker AXS) was used for the data evaluation. To quantify the transformation of aragonite into HAp the refinement was performed on the XRD patterns with known addition of Si. This method allowed us to follow quantitatively the HAp transformation kinetics as temperature and time functions of HT treatment. The same XRD patterns were used to determine the change of crystallite size of HAp along the *c* and *a*-axes applying the Scherrer approximation on (002) and (030) reflections. Johnson-Mehl-Avrami (JMA) kinetics model for nucleation and growth [15,16] was used. JMA model describes fraction of HAp formed as a time dependent function, α(t), and can be written as:

$$\alpha(t)= 1\text{-}\exp[-(kt)^n],$$

where the Avrami exponent, *n,* is a constant depending on the type of nucleation and growth process and *k* is crystallization rate constant involving both nucleation and crystallization parameters. Fourier transform infrared analysis (FTIR) was performed by attenuated total reflectance (ATR) spectroscopy for solids with a diamante crystal.

Results and discussion

XRD diffraction and kinetics of transformation

Powder X-ray diffraction analysis of cuttlebones heated at 350°C have shown that the external wall of cuttlebone is transformed completely into calcite, whereas the internal lamellae part of bones have aragonitic structure even after heat treatment at 350°C for 3 hours. Therefore for hydrothermal treatment only peaces of internal cuttlebone matrix (lamellae spacing) were used. The influence of hydrothermal treated temperature and time on the crystalline state of the produced scaffolds is shown in Fig. 1.

XRD patterns clearly show that at the beginning of heat treatment aragonite transforms rapidly into HAp, but 24 hours at 200°C and 48 hours at 180°C, respectively, were needed for complete transformation of aragonite into HAp. Diffraction data were analyzed using the Rietveld refinement approach [17], which allowed us to follow quantitatively the formation of HAp as functions of temperature and time of HT treatment. The HAp structure reported by Sundarsanan and Young [19] was used as a structural model in the Rietveld refinement, and the structural model for aragonite was taken from ICSD card 15-198. The scale factor, zero displacement, background coefficients, unit cell axes and profile function parameters were refined first. In the second step atomic positions and site occupancies were also refined, while the temperature displacements were kept fixed. The background was described by Chebishev polynomal, of 6th order and the diffraction profile was modeled by pseudo-Voigt peak-shape function.

Rietveld output of XRD data for sample HT treated at 200°C for 24 hours with 5 wt% of silicon as internal standard is given in Fig. 2 as an example.

The HAp quantity formed by HT treatment and the kinetics of transformation are shown in Fig. 3. As seen (right sided *y*-axis in Fig. 3), for 1 hour at 200°C about 50 wt%, and for the same time at 180°C about 35 wt% of HAp was formed. After treatment for 48 hours no aragonite was determined by XRD in the sample HT treated at 200°C, whereas in the sample treated at 180°C about 2 wt% of aragonite remained un-transformed. The fraction of crystallized HAp data (left sided *y*-axis in Fig. 3) were fitted to the Johnson-Mehl Avrami model for nucleation and growth and obtained constants were: k_{200}=0.58(2) h^{-1} and k_{180}=0.26(1) h^{-1}, respectively. The Avrami exponent was equal (n=0.57(3) and n=0.57(3), respectively), for both temperatures.

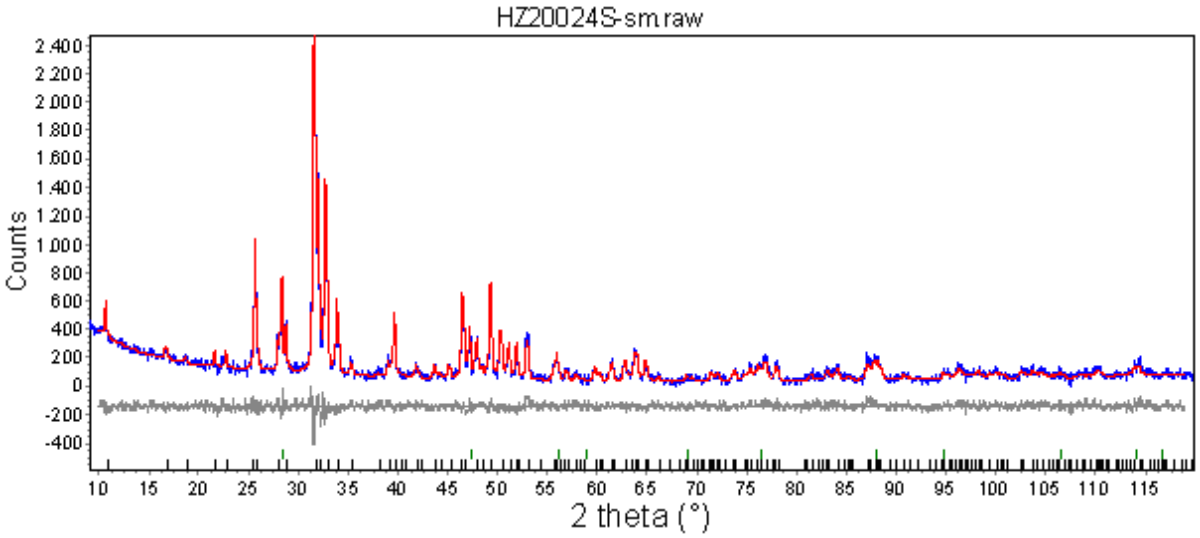

Fig. 2 Rietveld output of x-ray powder pattern of the sample heat-treated at 200°C for 24 hours. The dots are the experimental data, and the solid line is the best-fit profile. The difference between the experimental and fitted pattern is shown under the diffraction pattern. Line markers on the bottom of the figure indicate the positions of Bragg reflections for hydroxylapatite and Si. R_{exp}=8.51, R_{wp}=12.80, GoF=1.50.

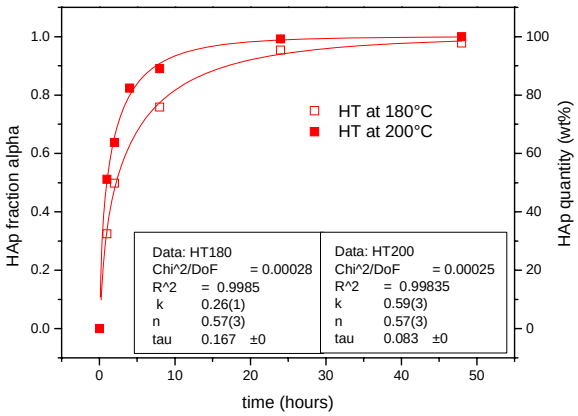

Fig. 3. α-t curves for HAP formed at 180°C and 200°C.

The change of crystallite size was followed using Scherrer equation and Si as a standard to correct the instrumental broadening. As shown in Fig .4, the crystallites size increases with the time of HT treatment up to about 24 hours. Longer treatment affects no increase of crystallite size along *a*-axis, and very small increase along the *c*-axis.

These results compared with the amount of formed HAp as a function of time (Fig. 3) suggest that its formation could be defined as diffusion controlled growth of crystals with the dominant growth along to the *c*-axis direction.

The changes of unit cell parameters of hydroxyapatite with time and temperature is shown in Fig. 5. There is some difference between the unit cell parameters of HAp formed at 180°C and 200°C. Samples heated at 180°C exhibited the both *a*–and *c*– axis larger than are those for HAp in samples treated at 200°C and larger than those for structurally well defined and pure hydroxyapatite [19]. With the time of HT treatment the parameters at 180°C are narrowing to those at 200°C, but even after heat treatment for 48 hours they are somewhat higher

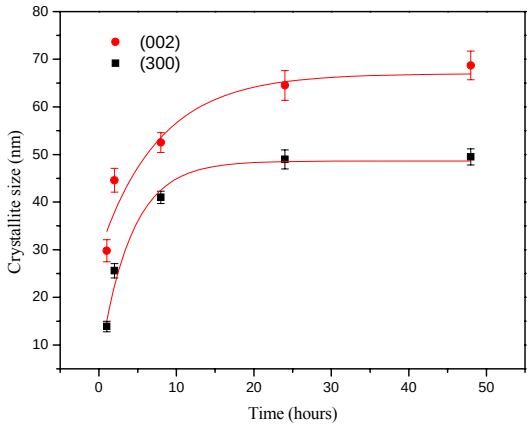

Fig.4. Evolution of Hap crystallite sizes along the *a=b* and c-axes, as a function of HT treatment at 200°C.

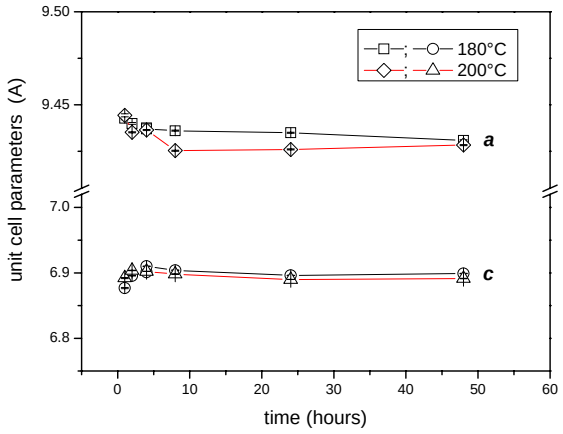

Fig. 5. Unit cell parameters of HAp as a function of temperature and time.

FT-IR spectroscopy

The FTIR spectra of HAp formed during the hydrothermal treatment are shown in Fig. 6 along to the spectrum of heated cuttlefish bone. The spectrum of cuttlefish bone reveals the IR active CO_3^{2-} bands of aragonite at 1446 (ν_3), 1082 (ν_1), 852 (ν_2), and doublet at 712, 710 cm^{-1} (ν_4) (Fig. 5A(b)).
The FTIR spectra of samples HT treated at 180°C show in the high energy region (Fig. 6A(a)) broad bands, which are related to stretching vibrations of H_2O. The small band assign to OH^- groups at 3575 cm^{-1} is first seen after HT treatment for 24 and 48 hours, respectively. At the same spectra the bending mode vibration of OH^- group at 630 cm^{-1} was also observed (Fig. 6A(b)). The formation of HAp by HT treatment is evident by fundamental vibrational modes of PO_4^{3-} tetrahedra (ν_3 at 1020-1086 cm^{-1} and ν_4 at 602 and 561 cm^{-1}) (Fig. 6A(b)). ν_1 vibrations of PO_4 at 960 cm^{-1} is evident after HT treatment for 1 hour. The presence of small amounts of aragonite even after HT for 48 hours (Fig. 1B) masks partially the bands attributed to carbonate in the HAp structure. There are two types of carbonate substitution in HAp. The carbonate groups substitute either at the phosphate tetrahedra (B-type), or at the hydroxyl sites (A-type) or both (A-B type). The carefully analysis of spectra indicates that CO_3^{2-} groups are preferentially incorporated on PO_4 tetrahedral sites as suggested by the vibration frequencies of CO_3^{2-} at 874 cm^{-1} for ν_2 and 1545, 1456, 1416 cm^{-1} for ν_3 bands The increasing of spectra resolution in conjunction with the increase of the sharpness and intensity of diffraction lines (Fig. 1B) indicate the increase of crystallinity of formed HAp. The spectra with frequencies between 1700 and 450 cm^{-1} suggest B-type incorporation of CO_3^{2-} groups. The spectra of samples HT treated at 200°C (Fig. 6B) show better resolution of frequencies. The band at 3575 cm^{-1} attributed to OH stretching mode (Fig. 6B(a)) is first observed after HT treatment for 2 hours. The spectra with frequencies between 1700 and 450 cm^{-1} (Fig. 6B(b)) suggest also B-type incorporation of CO_3^{2-} groups and structurally better defined HAp in shorter time.

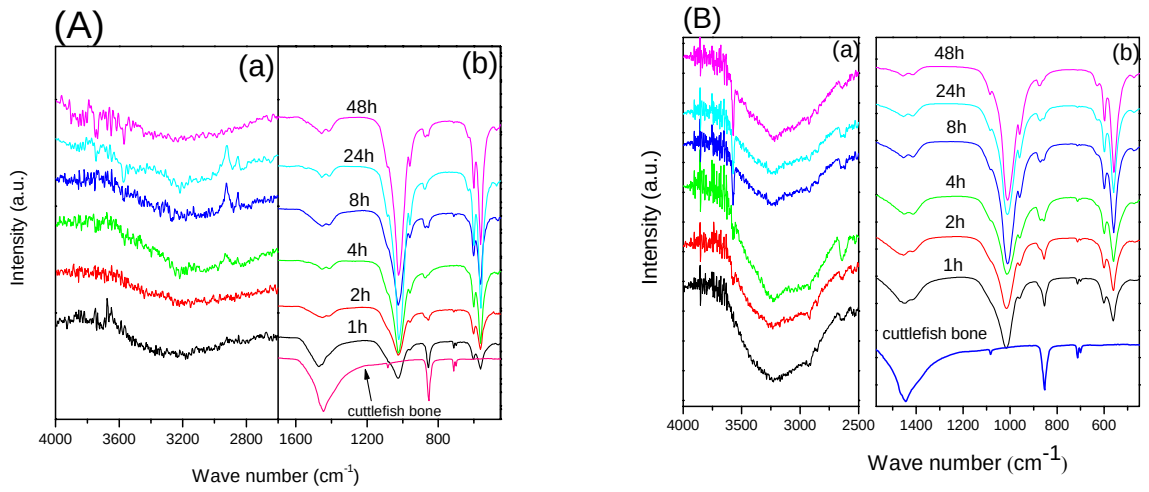

Fig. 6. FTIR spectra of transformed cuttlefish bone by HT treatment at: (A) 180°C and (B) 200°C. (a) high energy region, (b) frequences between 1700–450 cm^{-1}.

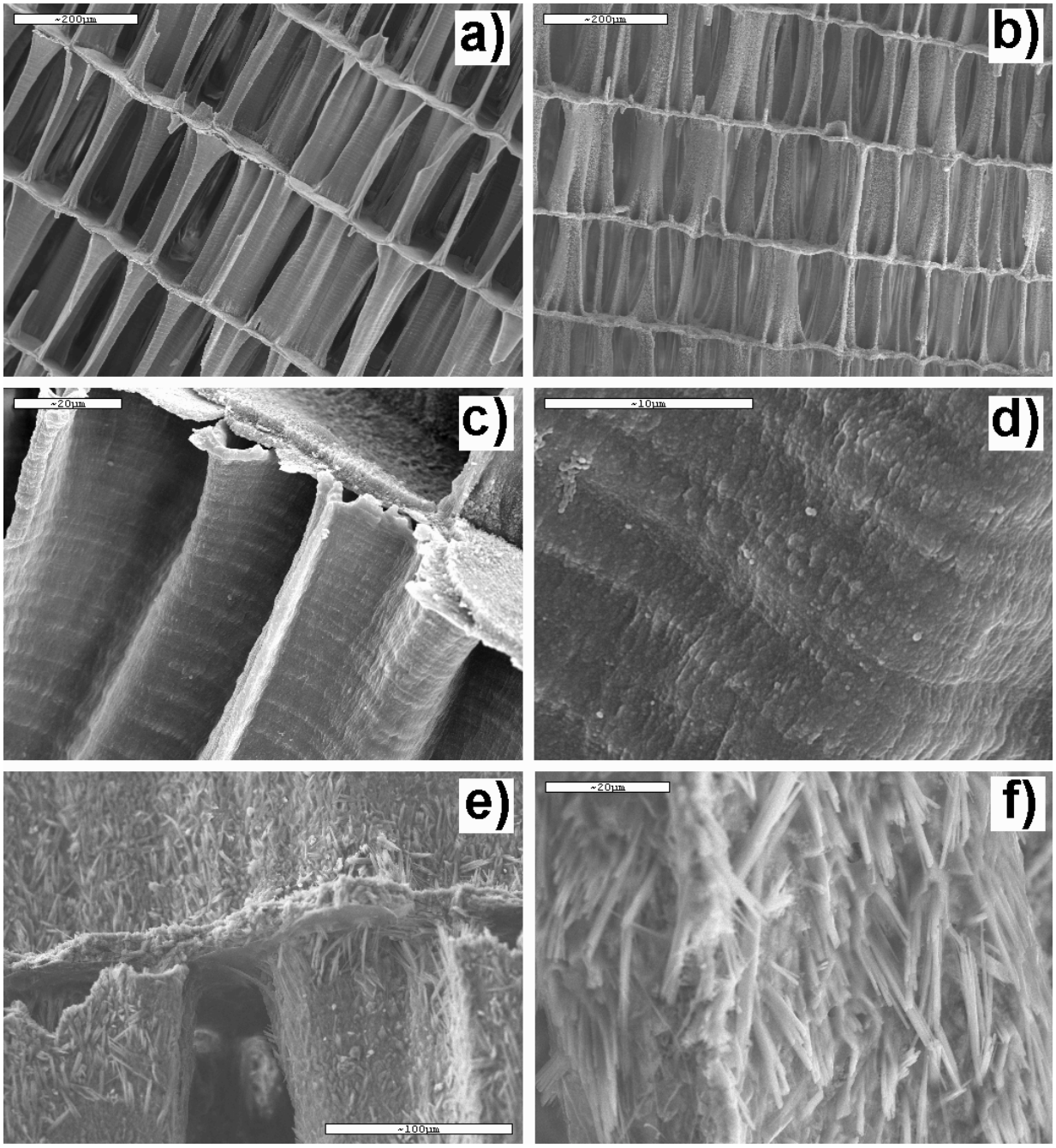

Fig. 7. SEM micrographs of cuttlefish bone: a) heat treated at 350°C for 3h; b) after hydrothermal conversion into HAp at 200°C for 24 hours; c) and d) higher magnifications of the picture a) representing the corrugate structure of pillars; e) and d) higher magnification of the picture b), from which the elongated crystals of HAp are seen.

Microstructure

The micrographs of cuttlefish bone HT treated at 200°C for 48 hours is shown in Fig. 7 in comparison with micrograph of the same bone before hydrothermal treatment. The parallel sheets (lamellae) supporting by transversal pillars form chambers, which are sealed from each other [20]. The spacing between lamellae is about 200 µm, as seen in Fig. 7a, but it varies in different areas of the bone; usually between 200 and 600 µm. The pillars have S-shape crossed-sections and the growth steps along the length of them are shown in Fig. 7c. The comparison of microstructure of heat-treated cuttlefish bone (Fig. 7a) with micrograph of completely transformed cuttlefish bone into HAp at 200°C for 24 hours (Fig. 7b) shows that the channeled architecture is completely preserved. Higher magnifications of pillars of heat-treated sample (Fig. 7e and 7f), clearly show needle-like HAp crystals that grow predominantly along the height of the pillars. .

Conclusion

The complete transformation of aragonitic cuttlefish bones into hydroxyapatite can be achieved by HT treatment at 200°C for 24 hours, whereas longer time is needed if the transformation was attained at lower temperatures.

The process can be described as diffusion controlled growth of needle-like crystals with higher growth in c-axis direction.

Unit cell parameters of HAp achieved at 200°C for 48 h match well with literature data, whereas higher parameters were obtained if the HT treatment were performed at lower temperatures.

FTIR spectra revealed incorporation of carbonate in the PO_4^{3-}-sites of HAp structure (B-type incorporation). The OH^- incorporation in the HAp structure depends on temperature and time of the HT treatment. At 200°C, the incorporation of OH^- groups in the structure is achieved after 2 hours, while at 180°C 24 hours is needed for formation of well defined hydroxyapatite.

The porous channeled architecture of aragonitic cuttlefish bones is completely preserved by HT treatment

Acknowledgment

The financial support of the Ministry of Science, Education and Sports of the Republic of Croatia in the frame of the project "Bioceramic, Polymer and Composite Nanostructured Materials", (No.125-1252970-3005). is gratefully acknowledged. Thanks are due to Universidad Politecnica de Valencia, Spain for the financial support to the author H.I. during his research study in Centro de Biomateriales.

References

1. L.L. Hench, J. Wilson: Introduction to bioceramics, Singapore World Scientific; 1993.
2. R.Z. LeGeros, J.P. LeGeros: Dense hydroxyapatite. In :Hench, L.L., Wilson J., editors. Introduction to bioceramics. Singapore, World Scientific; 1993. p 138-90.
3. J.H.G. Rocha, AF. Lemos, S. Agatholopoulos, P. Valerio, S. Kannan, F.N. Oktar, JMF. Ferreira Scaffolds for bone restoration from cuttlefish, Bone 37 [6] (2005) 850-857.
4. K. Yamashita, T. Kazanawa, in *Inorganic phosphate materials*, ed. T. Kazanawa, Elsevier, Amsterdam 1989.
5. C. E. Wilson, J.D. de Brujin, C.A. van Blitterswijk, A.J. Verbout, W. J. A. Dhert, Design and fabrication of standardized hydroxyapatite scaffold with a defined macro-architecture by rapid prototyping for bone-tissue-engineering research. J. Biomed. Mater. Res.. Part A 68A (2003) 123-132.
6. AF., Lemos, JMF., Ferreira: Designing of bioceramics with bonelike structures tailored for different orthopedic applications. Key Eng. Mater. 254-256 (2004), 1037-40.
7. E.C. Shors, R.E. Holmes, Porous hydroxyapatite. In Hench L.L., Wilson, J., editors. Introduction to bioceramics. Singapore, World Scientific; 2003, p.181-198.
8. A.F. Lemos, J. H. Rocha, S. S. F.Quaresma, S.Kannan, F. N. Oktar, S.Agathopoulos, J. M. F. Ferreira, Hydroxyapatite nano-powders produced hydrothermally from nacreous material- J. Eur. Ceram. Soc., 26 [16] 2006, 3639-3646
9. M. Ni, B.D. Ratner: Nacre surface transformation to hydroxyapatite in a phosphate buffer solution, Biomaterials 24 (2003), 4323-31.
10. J.H.G Rocha, AF. Lemos, S. Kannan, S. Agatholopoulos, JMF.Ferreira: Hydroxyapatite scaffolds hydrothermally grown from aragonitic cuttlefish bones, J. Mater. Chem. 15 [47] (2005), 5007-5011.
11. J.H.G. Rocha, AF. Lemos, S. Agatholopoulos, Kannan, S., Valerio, P., Ferreira, JMF., Hydrothermal growth of hydroxyapatite scaffolds from aragonitic cuttlefish bones. Journal of Biomedical Materials Research, Part A 77A, [1] (2006), 160-168.
12. W. Eysel and D.M. Roy, Z. Kristallogr., Bd 141 (1975). 11-24.
13. C. M. Zaremba, D.E.,Morse, S. Mann, P.K. Hansma, G.D. Stucky: Chem. Mater. 10 (1998), 3813-3824.
14. M. Yoshimura, P. Suyaridworakun, F. Koh, F. Fujiwara, D. Pongkau, A. Ahniyaz: Hydrothermal conversion of calcite crystals to hydroxyapatite. Mater. Sci. & Eng. C 24 (2004), 521-524
15. W.A. Johnson, R.F. Mehl Trans. Am. Inst. Min. Eng. 135(1939), 416.
16. M.J. Avrami. Chem. Phys.9 (1941), 177.
17. R.A. Young, The Rietveld Method, International Union of Crystallography. Monographs on Crystallography, Vol. 5. Oxford Press, Oxford, 1993.
18. Bruker AXS, Advanced X-Ray Solutions, TOPAS2-1, 2003.
19. K. Sundarsanan, Young R.A., Significant precision in crystal structural details: Holly Springs hydroxyapatite. Acta Crystallogr. B 25 (1996), 1534-43.
20. Birchall, J.D., Thomas, N.L., On the architecture and function of cuttlefish bone. J. Mater. Sci. 18 (1983) 2081-2086.